Capturing Truthiness: Mining Truth Tables in Binary Datasets

Clifford Conley Owens, T. M. Murali, and Naren Ramakrishnan
Department of Computer Science, Virginia Tech, VA 24061, USA
Email: {ibcliffo,murali,naren}@cs.vt.edu

ABSTRACT

We introduce a new data mining problem: mining truth tables in binary datasets. Given a matrix of objects and the properties they satisfy, a truth table identifies a subset of properties that exhibit maximal variability (and hence, complete independence) in occurrence patterns over the underlying objects. This problem is relevant in many domains, e.g., bioinformatics where we seek to identify and model independent components of combinatorial regulatory pathways, and in social/economic demographics where we desire to determine independent behavioral attributes of populations. Besides intrinsic interest in such patterns, we show how the problem of mining truth tables is dual to the problem of mining redescriptions, in that a set of properties involved in a truth table cannot participate in any possible redescription. This allows us to adapt our algorithm to the problem of mining redescriptions as well, by first identifying regions where redescriptions cannot happen, and then pursuing a divide and conquer strategy around these regions. Furthermore, our work suggests dual mining strategies where both classes of algorithms can be brought to bear upon either data mining task. We outline a family of levelwise approaches adapted to mining truth tables, algorithmic optimizations, and applications to bioinformatics and political datasets.

Categories and Subject Descriptors: H.2.8 [Database Management]: Database Applications - Data Mining; I.2.6 [Artificial Intelligence]: Learning

General Terms: Algorithms.

Keywords: truth tables, levelwise algorithms, independence models.

1. INTRODUCTION

Consider the dataset shown in Fig. 1(a), which outlines nine hypothetical senators and their votes (1 for yes, 0 for no) on four bills. Given binary matrices such as these, our goal in this paper is to identify a truth table embedded inside them. Our first observation is that, given nine rows, we can find truth tables having at most $\lfloor \log_2(9) \rfloor = 3$ bills. However, the reader can verify that no such truth table exists. In fact, the only two truth table present is a two-column one, spanning the bills 'War' and 'Tax Cuts,' as shown in Figure 1(b). This truth table suggests that these two bills constitute independent dimensions along which politicians distinguish themselves. Observe that the senators partition into four (2^2) disjoint subsets with each subset having at least two senators. We separate these subsets using dashed lines in Figure 1(b).

This problem of finding truth tables can be considered orthogonal to mining association rules [1], correlations [21], or redescriptions [13] which capture various forms of attribute dependencies and overlaps. From the perspective of these works, truth tables constitute an 'anti-pattern,' i.e., the variables participating in it defy similarity judgements, and are hence interesting. (Later we show how truth tables can be harnessed to find patterns of similarity as well).

Several application domains possess characteristics that are amenable to truth table mining. In bioinformatics, we are given a matrix of genes (rows) versus transcription factors (columns), where a 1 indicates that the transcription factor binds upstream of the given gene, and regulates it (0 otherwise). A truth table in such a matrix indicates a set of transcription factors that can be recruited in arbitrary combinations to regulate genes. This further suggests that they are likely to form independent components of regulatory pathways. Similar relationships underlie signaling pathway analysis [10] and exploration of therapies for drug discovery [3].

As a second example, consider the domain of recommender systems where the rows denote people, the columns denote movies, and a 1/0 indicates approval/disliking (assume for now that everybody has seen and rated every movie). When a new person joins the system, a typical problem faced in recommenders is to identify a (small) set of movies that this new person should be requested to rate, in order to be connected to the underlying social network of users. By identifying a truth table in the original matrix, we can learn a set of movies that serve to maximally distinguish a user from others, and hence situate the user in a suitable neighborhood. Thus, the ratings for these movies are the most informative questions to ask a new user. This application directly maps to recommender system designs like Jester [6] which request all users to rate the same set of artifacts. Truth table mining identifies what these artifacts should be.

A truth table can be viewed as a partition of rows where each block in the partition is a 'constant-row' bicluster [9].

KDD'07, August 12–15, 2007, San Jose, CA, USA.

	War	Electoral Reforms	Tax Cuts	Environmental Reforms
Adam	1	0	0	0
Bill	1	0	1	1
Clinton	0	0	1	1
Dwight	0	0	1	1
Edwards	0	1	0	1
Frank	0	1	0	1
Ganguly	0	0	0	1
Hildebrand	0	1	1	1
Ironside	0	0	0	1

(a) The voting records of nine senators on four bills.

	Electoral Reforms	**War**	**Tax Cuts**	Environmental Reforms
Edwards	1	**0**	**0**	1
Ganguly	0	**0**	**0**	1
Ironside	0	**0**	**0**	1
Clinton	0	**0**	**1**	1
Dwight	0	**0**	**1**	1
Adam	0	**1**	**0**	0
Frank	0	**1**	**0**	1
Bill	0	**1**	**1**	1
Hildebrand	0	**1**	**1**	1

(b) Rearranged matrix from (a) revealing a truth table formed by voting patterns on 'War' and 'Tax cuts'.

Figure 1: Example dataset for truth table mining.

The most familiar type of constant-row patterns are those where all cells are 1, and such biclusters correspond to itemsets as studied in association mining. Hence algorithms for mining truth tables must explicitly and necessarily keep track of an exponentially greater number of occurrence patterns than algorithms for mining associations. At the same time, truth tables expose several structural constraints that can be harnessed to create effective algorithms. In particular, although the definition of the underlying pattern is more complicated, we show how the search for truth tables can be structured levelwise, drawing upon established notions from data mining.

"Truthiness" [20] is a term coined by television comedian Stephen Colbert to describe things that a person claims to know intuitively, instinctively, or "from the gut." The Newspeak word "bellyfeel" [19] has similar connotations. The truth tables we compute have high truthiness, which we capture using two parameters: (i) we insist that each pattern of occurrences occur in as many rows as demanded by a *balance* criterion; (ii) however, we allow a small number of patterns to appear in fewer rows, controlled using the *support* parameter. More information on these parameters is provided in Section 2.

Our main contributions in this paper are:

1. We formulate truth table mining as a new data mining task, with associated algorithms and applications. We define the notions of balance and support to characterize the quality of a truth table. These notions smoothly decrease with an increase in the number of properties in a truth table.

2. We give theoretical insights into the relationships between truth tables and redescriptions [22] and cast these as duals of each other. This allows us to adapt insights from algorithms for mining one type of pattern toward mining the other type of pattern.

3. We present experimental results on both synthetic and real-world datasets, helping demonstrate the scalability of our implementation and also shedding domain-specific insight.

Section 2 formally defines the truth table mining problem and Section 3 outlines how our definitions of balance and support lend themselves to levelwise search algorithms. Section 4 describes the levelwise algorithm in detail, along with some associated optimizations for improving efficiency. Section 5 presents relationships to redescription mining and outlines the context in which it is dual to truth table mining. Section 6 gives experimental results on both synthetic and real-world datasets. Sections 7 and 8 provide comparisons to related work and offer a discussion, respectively.

2. PROBLEM FORMULATION

Let O denote a set of n objects, P a set of m properties, and $R \subseteq O \times P$ a relation that connects objects to properties they contain. We are interested in identifying complete independence in the occurrence of subsets of P among the objects in O. Let $Q \subseteq P$ denote a subset of properties. Given any object $o \in O$, let o_Q denote the binary vector with $|Q|$ elements given by the values of the properties in Q in o.Since there are $2^{|Q|}$ possible distinct values of this binary vector, Q partitions the objects in O into at most $2^{|Q|}$ equivalence classes. Let E_Q denote this partition. Each element of E_Q is a set of objects and each object appears in precisely one element of E_Q. A *truth table* is a pair (Q, E_Q), where $Q \subseteq P$ and $|E_Q| = 2^{|Q|}$.

Note that if no two properties in P are identical (i.e., both properties appear in precisely the same set of objects), a truth table (Q, E_Q) is naturally closed: by definition, the truth table includes all objects and any property in $P - Q$ will induce a refinement of E_Q if added to Q. Henceforth, we will abuse notation and use Q to refer both to a subset of properties and the induced truth table.

Truth tables have natural notions of balance and support, which we define next. Ideally, in a truth table (Q, E_Q), each subset of objects in E_Q will have size at least $\lfloor n/2^{|Q|} \rfloor$. To accommodate deviations from this ideal, we define the *balance* $\beta(Q)$ of (Q, E_Q) to be the quantity

$$\beta(Q) = \frac{\min_{S \in E_Q} |S|}{n}.$$

Thus, every element of E_Q contains at least $\beta(Q)n$ objects. Values of balance range between 0 and $1/2^{|Q|}$. Given a balance threshold $0 \leq b \leq 1$, we say that a truth table Q is *balanced* if $\beta(Q) \geq b$. As we will show in the next two sections, our definition of balance is anti-monotone, a property we exploit in our truth table mining algorithms.

Observe that we could have defined balance in a way that normalised it with respect to the number of properties in Q, e.g., $\beta(Q) = \frac{\min_{S \in E_Q} |S|}{n/2^k}$. In this case, although $\beta(Q)$ ranges between 0 and 1, it does not exhibit anti-monotonicity. In particular, a version of Lemma 3.2 below does not hold for this definition.

We also desire to mine 'almost truth tables,' where most, but not all, of the presence/absence combinations of properties satisfy the balance constraint. Given a balance threshold b, we define the *support* $\sigma(Q, b)$ of a truth table (Q, E_Q) with balance at least b to be the fraction of possible object sets whose size is at least bn, i.e.,

$$\sigma(Q, b) = \frac{|\{S \in E_Q, |S| \geq bn\}|}{2^{|Q|}},$$

where $2^{|Q|}$ is the maximum possible number of object sets in E_Q. Given a support threshold $0 \leq s \leq 1$, we say that a balanced truth table Q is *supported* if $\sigma(Q, b) \geq s$.

We illustrate the notions of balance and support using the data in Figure 1. For example, the balance of the truth table formed by the bills 'War' and 'Tax Cuts' in Figure 1(b) is 2/9 and its support is 1. A two-bill truth table in this dataset (with nine senators) cannot have balance greater than 2/9: such a truth table partitions the senators into four groups, one of which must contain at most two senators. If we were to form a truth table involving the bills on 'War,' 'Tax Cuts,' and 'Environmental Reforms', we note that of the eight expected groups of senators, only five occur in this dataset. One of these groups has size three (senators Edwards, Ganguly, and Ironside), two groups have size two (Clinton-Dwight and Bill-Hildebrand), and the other two groups have one senator each. Thus, with a balance threshold of 1/9, this truth table has a support of 5/8. If we increase the balance threshold to 2/9, then the support of the truth table drops to 3/8.

Thus, the pair of values (b, s) together characterise the "truthiness" [20] of desirable truth tables. An ideal truth table (say, one with k properties) has balance $\lfloor 1/2^k \rfloor$ and support equal to 1. However, any truth table with high balance and high support also "feels like a real truth table in the gut," a phenomenon that is the hallmark of truthiness.

Given a set O objects, a set P of properties, a relation $R \subseteq O \times P$ that connects objects to properties they contain, a balance threshold $0 \leq b \leq 1$, and a support threshold $0 \leq s \leq 1$, the *truth table mining problem* is the task of computing all truth tables Q in R with $\sigma(Q, b) \leq s$.

3. PROPERTIES OF TRUTH TABLES

We now prove a series of lemmas that establish the anti-monotone properties of balance and support. We also list some properties of balanced and supported truth tables that lead to algorithmic optimisations in the computation of truth tables. First, we define some useful notation. In a truth table Q, let $U_Q \subset E_Q$ be the set of object sets with size less than bn, i.e., those that do not satisfy the balance constraint. Consider two truth tables Q' and Q such that $Q' \subset Q$ and Q contains one more property than Q'. Consider any object set S in $E_{Q'}$. In Q, this object set partitions into two object sets, depending on whether the new property is present or not in the objects in S. Call them S_1 and S_2. We refer to S as a *parent* of S_1 and S_2. Note that S_1 and/or S_2 may be empty. Figure 2 illustrates this notion.

Our first lemma, which we state without proof, simply states that as we include more properties in a truth table, the support cannot increase.

LEMMA 3.1. *If Q and Q' are two truth tables with $Q \subset Q'$, then $\sigma(Q, b) \geq \sigma(Q', b)$.*

The next lemma establishes the anti-monotonicity of balance and support.

LEMMA 3.2. *If a truth table Q has balance b and support s, then every truth table $Q' \subseteq Q$ such that $|Q'| = |Q| - 1$ has balance b and support s.*

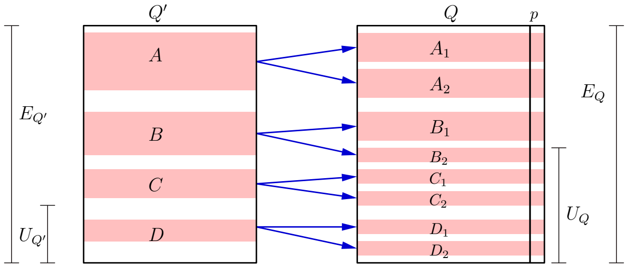

Figure 2: An example of a truth table Q' with $k-1$ properties and a truth table Q that contains an additional property p.

Figure 2 illustrates the ideas used in the proof. In this figure, vertical lines denote the extent of $E_{Q'}$, E_Q, $U_{Q'}$, and U_Q. Shaded rectangles denote object sets. The figure indicates that the object set

1. $A \in E_{Q'} - U_{Q'}$ is the parent of $A_1, A_2 \in E_Q - U_Q$,
2. $B \in E_{Q'} - U_{Q'}$ is the parent of $B_1 \in E_Q - U_Q$ and $B_2 \in U_Q$,
3. $C \in E_{Q'} - U_{Q'}$ is the parent of $C_1, C_2 \in U_Q$, and
4. $D \in U_{Q'}$ is the parent of $D_1, D_2 \in U_Q$.

PROOF. Let Q have k properties. By the definition of support, $|U_Q| \leq (1 - s)2^k$. Let Q' be a truth table such that $Q' \subseteq Q$ and $|Q'| = k - 1$. Consider any object set S in $E_{Q'}$. There are three cases to consider:

(i) $S \in U_{Q'}$ (e.g., object set D in Figure 2): Since $|S_1|, |S_2| \leq |S| \leq bn$, both S_1 and S_2 are elements of U_Q.

(ii) $S \in E_{Q'} - U_{Q'}$ and both S_1 and S_2 have size at least bn (e.g., object set A in Figure 2): both S_1 and S_2 are elements of $E_Q - U_Q$.

(iii) $S \in E_{Q'} - U_{Q'}$ and at least one of S_1 or S_2 has size less than bn (e.g., object set C in Figure 2).

Let x be the number of object sets in U_Q whose parent is in $E_{Q'} - U_{Q'}$. The number of such parents is at most x. Therefore, we have the following inequality:

$$|U_Q| = 2|U_{Q'}| + x \leq (1 - s)2^k.$$

Since $x \geq 0$, we have $|U_{Q'}| \leq (1 - s)2^{k-1}$, which implies that Q' has balance b and support s. $\square$

Note that if we had defined the balance of a truth table Q as $\beta(Q) = \frac{\min_{S \in E_Q} |S|}{n/2^k}$, this lemma may not hold. In particular, if the truth table Q' in the proof has $\sigma(Q', b) < s$, any object set $S \in U_{Q'}$ has size less than $bn/2^{k-1}$. However, one of the object set S partitions into in E_Q may have size at least $bn/2^k$, thus enabling $\sigma(Q, b)$ to be at least s, violating the desired anti-monotonicity.

LEMMA 3.3. *Let Q be a truth table with k properties, balance b and support 1. If there is at least one object set in E_Q with size less than $2bn$, then every truth table $Q' \supset Q$ with balance b has support strictly less than 1.*

PROOF. Let S be the offending object set in E_Q. Let $Q' \supset Q$ be a truth table with $k+1$ properties. The object set S is the parent of two object sets S_1 and S_2 in $E_{Q'}$. Since $|S| < 2bn$, at least one of S_1 or S_2 must have size less than bn, which implies that Q' does not have support 1. □

The previous lemma implies a stronger form of the anti-monotone property guaranteed by Lemma 3.2 for the case when the support is 1.

COROLLARY 3.4. *If Q is a truth table with k properties, balance b and support 1, then every sub-truth table of Q with $k-1$ properties has balance $2b$ and support 1.*

We can generalise the previous lemma to all values of support s.

LEMMA 3.5. *Let Q be a truth table with balance b and support s. Suppose that there are l_Q object sets in E_Q with size at least bn and $2bn$ and that there are v_Q object sets in E_Q with size at least $2bn$. If $l_Q + v_Q < s2^{k+1}$, then every truth table that contains the properties in Q and has balance b has support strictly less than s.*

PROOF. Consider any truth table $Q' \supset Q$ with $k+1$ properties. Consider any of the $l_Q - v_Q$ object sets in E_Q with size between bn and $2bn$; each such object set is the parent of at most one object set in $E_{Q'}$ whose size is at least bn. An example is object set B in Figure 2. Each of the v_Q object sets in E_Q with size at least $2bn$ is the parent of at most two object sets in $E_{Q'}$ whose size is at least bn. All other object sets in E_Q are elements of U_Q. Hence, they are parents of object sets in $U_{Q'}$. Therefore $E_{Q'}$ can contain at most $l_Q - v_Q + 2v_Q = l_Q + v_Q$ object sets with size at least bn. If $l_Q + v_Q < s2^{k+1}$, then $\sigma(Q', b) < s$. □

4. MINING TRUTH TABLES

Since our balance and support constraints apply anti-monotonically (see Lemma 3.2), we present a simple level-wise algorithm, *a la Apriori*, to find all truth tables in a relation that satisfy given balance and support constraints. For each $k \geq 1$, given all truth tables with k properties, we construct candidate truth tables with $k+1$ properties. We use the heuristic of generating candidate truth tables at level k by merging two balanced and supported truth tables at level $k-1$ such that they share $k-2$ properties in common [1] (we encapsulate this step in the GENERATE-CANDIDATES subroutine, which is identical to the one in the Apriori algorithm [1]). For each candidate truth table T, we check if every sub-truth table of T with k properties satisfies the balance and support constraints. Finally, we perform one pass over the relation to compute the balance and support of each candidate truth table. We output only those candidates that satisfy these constraints.

Any truth table Q with k properties that satisfies $\sigma(Q, b) \geq s$ must contain at least $s2^k$ non-empty row subsets in E_Q. Since a trivial bound on the size of E_Q is n, the number of objects in O, we see that no truth table can contain more than $\lceil \log(n/s) \rceil$ properties.

Algorithm 1 FINDTRUTHTABLES(O, P, R, b, s):

Input: A relation R relating objects in O to properties in P, a balance threshold $0 \leq b \leq 1$ and a support threshold $0 \leq s \leq 1$.

Output: All truth tables T such $\sigma(T, b) \geq s$.

```
𝒯 ← {p ∈ P | σ({p}, b) ≥ s}
while 𝒯 is not empty do
  for every truth table T ∈ 𝒯 do
    for every truth table T′ ⊆ T, |T′| = |T| − 1 do
      if σ(T′, b) < s then
        Discard T
      end if
    end for
    Compute σ(T, b)
    if σ(T, b) ≥ s then
      Output T
      Insert T into 𝒯
    end if
  end for
  𝒯 ← GENERATE-CANDIDATES(𝒯)
end while
```

	P_1	P_2	P_3
o_1	0	0	0
o_2	1	0	1
o_3	1	1	0
o_4	0	1	1

Figure 3: Example dataset for illustrating relationships between truth tables and redescriptions.

In each outer loop, we efficiently compute $\sigma(T, b)$ for every truth table T in the current set of candidates $\mathcal{T}$, as follows. Suppose we are currently processing candidates with k properties. Recall that for an object $o \in O$, o_Q denotes the binary vector with $|T|$ elements given by the values of the properties in T in o. We consider o_Q to be a number in binary notation. For each truth table $T \in \mathcal{T}$, we maintain $2^k + 2$ quantities:

(i) $c_{T,i}, 0 \leq i < 2^k$ counts the number of objects $o \in O$ such that $o_T = i$,

(ii) $l_T = |\{c_{T,i}, 0 \leq i < 2^k \mid c_{T,i} \geq bn\}|$, i.e., the number of object sets in E_T with size at least bn, and

(iii) $v_T = |\{c_{T,i}, 0 \leq i < 2^k \mid c_{T,i} \geq 2bn\}|$, i.e., the number of object sets in E_T with size at least $2bn$.

As we read the properties contained in each object o from R, we compute o_T and update the corresponding values. Assume $o_T = i$. After incrementing $c_{T,i}$, we increment l_T if $c_{T,i}$ equals bn or we increment v_T is $c_{T,i}$ equals $2bn$. After we finish processing R, we can compute $\sigma(T, b)$ as l_T/n.

Computing v_T allows us to exploit Lemma 3.5 to prune our search further. If $l_T + v_T < s2^{k+1}$, then we know that for any truth table T' that contains the properties in T, $\sigma(T', b) < s$. We can remove T from the list $\mathcal{T}$used to generate candidates for the next level.

5. RELATIONS TO REDESCRIPTIONS

We now outline relationships between truth tables and redescriptions. Redescriptions are a newly introduced class of data mining patterns [13] that establish similarity relationships between general boolean formulae.

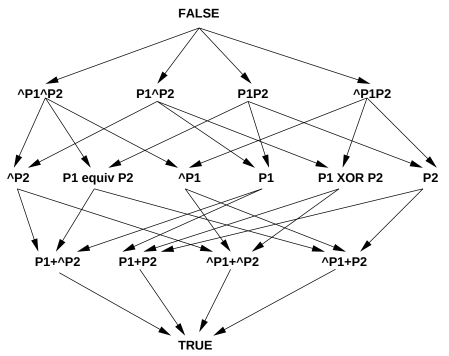

Figure 4: A relaxation lattice over expressions involving two boolean variables.

Consider as before relation $R \subseteq O \times P$; a *descriptor* over P is a boolean expression on a set of properties $V \subseteq P$. Given a descriptor e, we will denote the set of objects for which e is true (for a presumed R) by $O(e)$. Two descriptors e_1 and e_2 defined over (resp.) V_1 and V_2 are *distinct* (denoted as $e_1 \neq e_2$), if one of the following holds: (i) $V_1 \neq V_2$, or (ii) there exists some R for which $O(e_1) \neq O(e_2)$. Note that this condition rules out tautologies. For instance, the descriptors $P_1 \cap P_2$ and $P_1 - (P_1 - P_2)$ are not distinct. A descriptor e' is a *redescription* of e if and only if $e \neq e'$ and $O(e) = O(e')$ holds for the given R. In this case, we say that $e \Leftrightarrow e'$.

Observe that redescriptions subsume association rules in expressive power, since they generalize implications to equivalences. Every (100% confident) association rule can be restated as a redescription but not the reverse. For instance, the association rule $P_1 \rightarrow P_2$ (i.e., objects that have property P_1 also have property P_2) is equivalent to the redescription $P_1 \Leftrightarrow P_1 \cap P_2$ (i.e., objects that have property P_1 are the same as the objects that have both of properties P_1 and P_2).

Consider the artificial dataset shown in Figure 3 with four objects and three properties. Let us attempt to identify redescriptions by enumerating all possible boolean expressions and, for simplicity, focus on only the two properties P_1 and P_2. We know that two properties can induce 2^{2^2} boolean expressions, which can be arranged in a relaxation lattice as shown in Fig. 4. In this lattice, we have an arrow from expression e_1 to e_2 iff e_1 entails e_2, i.e., iff $\neg e_1 \vee e_2$ is a tautology; we then say that e_2 is a *relaxation* of e_1. Observe that the relaxation relation is dataset-agnostic, whereas redescriptions are not.

To mine redescriptions between expressions in Fig. 4, we assess if two or more of them induce the same object set. The reader can verify that, in fact, all 16 boolean expressions induce all possible $2^4 = 16$ subsets of objects from Fig. 3, and hence there are no possible redescriptions in this dataset! This is because the two properties P_1 and P_2 form a truth table over the given objects.

We have thus shown, by means of an example, that a dataset that induces a truth table of support 1 (i.e., all bitwise combinations are present) cannot induce redescriptions. The reader can verify that the balance parameter is not relevant for this relationship, as long as it is non-zero. We hence state the following (for a proof, see [11]):

THEOREM 5.1. *Let $R \subseteq O \times P$ be a relation between n objects and m properties such that each of the possible 2^m presence/absence combination of properties is observed in R. Let e be a descriptor over P. Then e has no redescription with any other descriptor defined over P.*

To make the analogy more concrete, consider what happens when we delete a single row from the dataset in Fig. 3, say the last row. When we delete row o_4, we see noticeable changes in the landscape of redescription terrains (Figure 5 (left)). Now, not only do redescriptions happen, every possible expression has a redescription! For instance, we obtain the redescription $P_1 \Leftrightarrow P_1 + P_2$ where the + symbol denotes logical OR, or union. This redescription states that objects that have either P_1 or P_2 (or both) are the same as objects that have P_1. Observe that this results because we deleted object o_4, the only object that had P_2 but not P_1. Similarly, the redescription P_1 AND $P_2 \Leftrightarrow P_1$ XOR P_2 results for the same row deletion.

THEOREM 5.2. *Let $R \subseteq O \times P$ be a relation between n objects and m properties such that at least one of the possible 2^m presence/absence combination of properties is not observed in R. Then every descriptor e over P has a redescription $e' \neq e$.*

As more rows are deleted, we observe a progressive, systematic, halving of the number of equivalence classes, as depicted in Figure 5 (middle, right).

COROLLARY 5.3. *Let $R \subseteq O \times P$ be a relation between n objects and m properties such that κ of the possible 2^m presence/absence combination of properties are not observed in R. Then every descriptor e over P has $2^\kappa - 1$ distinct redescriptions.*

The net effect of the above results culminates in:

THEOREM 5.4. *(Dichotomy Law) Let $R \subseteq O \times P$ be a relation between n objects and m properties. Then either no expression e over P has a distinct redescription or all expressions e over P have distinct redescriptions.*

(Although this theorem makes mining redescriptions appear to be a fruitless exercise, the task becomes interesting if we restrict the form of e, e.g., to be monotone, or to be conjunctions, in which case the dichotomy law doesn't hold, and the problem becomes non-trivial.) Returning to the example in Fig. 3, it is clear that, since every pair of columns induces a truth table, no redescriptions are possible between P_1 and P_2, between P_2 and P_3, and between P_1 and P_3. Nevertheless, there are redescriptions possible between all three of them, since the set of three properties does *not* induce a truth table. For instance, the redescription $P_1 \cup P_2 \Leftrightarrow P_2 \cup P_3$ holds. This suggests that the algorithm presented in this paper can be combined with the one described in [11] (that identifies redescription terrains) to fruitfully complement each other. The truth table miner can suggest to the redescription miner to directly proceed to expressions involving all three variables. Similarly, the redescription miner can suggest to the truth table miner that it is not worthwhile to proceed beyond level 2 in its levelwise search. This helps create a dual mining strategy to model either class of patterns. This approach is akin to algorithms such as Pincer search [8] that maintain two borders of patterns.

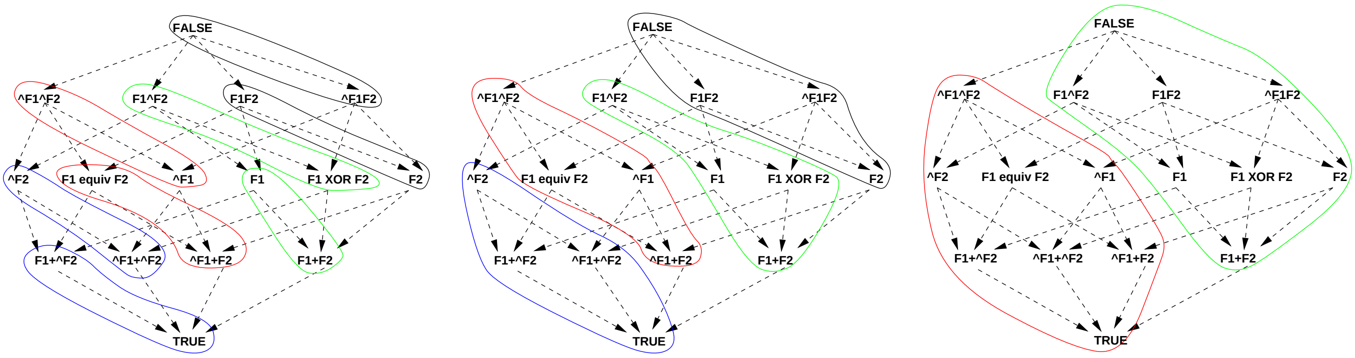

Figure 5: Redescription terrains form as rows are successively deleted from a truth table. (left) one row deletion, (middle) two row deletions, and (right) three row deletions. The redescription terrains displayed as closed curves are based on the data shown in Fig. 3 restricted to the first two columns F_1, F_2. The first figure uses rows o_1, o_2, o_3. The middle figure uses rows o_1, o_2. The right figure uses o_1.

6. APPLICATIONS

We present our results in three parts. First, we perform a comprehensive analysis of the ability of our algorithm to recover a truth table planted in a random binary matrix. Next, we discuss how our method unravels complex features of the network regulating gene expression in a cell. Finally, we mine voting patterns of U.S. senators to detect patterns of independence among them. Due to space constraints, we chose to highlight different aspects of our algorithm in these case studies: (i) synthetic data: scalability and the effect of dataset characteristics on algorithm running time; (ii) gene expression regulation: effect of balance and support thresholds on running time as well as truthy nuggets of discovered knowledge; (iii) senatorial voting patterns: statistical independence of properties in a truth table and domain-specific insights.

6.1 Synthetic Data

To systematically study the ability of our algorithm to find truth tables, we planted them in random binary matrices and tested the ability of our algorithm to discover the planted truth tables. We first describe our protocol in detail. We constructed random matrices based on three parameters k, r, and p. Note that these values are parameters for the simulation and not for the truth table mining algorithm. For each such triple, we perform the following steps:

1. Generate a binary matrix M with k columns and 2^k rows.
2. Select a random integer r, where $2 \leq r \leq k$, and plant a truth table with r columns in M. The truth table has balance $1/2^r$ and support 1. The r columns are interspersed randomly among the columns on M.
3. Set every element of M not belonging to the truth table to be a 1 with probability p and a 0 with probability $1-p$.
4. Execute the truth table finding algorithm on M with $b = 1/2^r$ and $s = 1$.

We executed these steps 10,000 times for the following choices of parameters: $k \in \{5, 10, 15, 20, 25\}$, five random values of r, and 11 values of p between 0 and 1 in increments of 0.1 For every (k, r, p) triple, we computed the average running time of our algorithm.

Our algorithm successfully recovered the planted truth table in every case. Therefore, in this section, we focus on presenting various slices of the three-dimensional function defined by the k, r, p and t (denoting time) values. A key feature of these results is the symmetric dependence of the running time on p. Unlike itemset and association rule mining algorithms, whose running time increases with p, the performance of our truth table mining algorithm is worst for $p = 0.5$ and symmetrically reduces around this value.

Dependence on p. Figure 6 displays how the running time of our algorithm depends on the probability p. Each plot in the figure corresponds to a fixed value of k. Each curve in a plot represents a fixed value of r. Due to lack of space, we only plot values for $k = 5$ and $k = 10$. As expected, these plots are symmetric around the line $p = 0.5$. For all values of k, the plot for $r = k$ is a nearly horizontal line, which is to be expected since the truth table spans the entire matrix.

Observe that in Figure 6(a) (where $k = 5$), the curve for any value of r dominates the curves for all smaller values of r. However, the behaviour is subtly different for $k = 10$ (Figure 6(b)). Whereas the curves for the range $r = 2$ to $r = 7$ follow this trend, none of the curves for $r = 7, 8, 9$, and 10 dominate each other. In particular, focus on $r = 7$ and $r = 8$. The curve for $r = 7$ dominates the curve for $r = 8$ for values of p approximately between 0.4 and 0.6. We further examine this apparent discrepancy below.

Dependence on k. Next, we examined how the running time varied with the number of columns k in the matrix, for fixed values of p. We fixed $k = 10$, since this case exemplifies higher values of k as well. Each plot in Figure 7 corresponds to a fixed value of p. We show the plots only for $p \leq 0.5$, because of symmetry. Consider Figure 7(a), where $p = 0$. The larger the value of the size of the planted truth table (r), the greater the running time of the algorithm. Now consider the other extreme $p = 0.5$ (Figure 7(f)). The running time has an inflection point at $r = 7$.

The running time of our algorithm on these synthetic datasets is primarily composed of two factors: 1. the time taken to discover the planted truth table and 2. the time spent in processing properties that do not belong to the planted truth table. The first component monotonically increases with r whereas the second component is influenced both by $k - r$ and by p. The second component is not monotonic in r. In this case, the contribution of the second com-

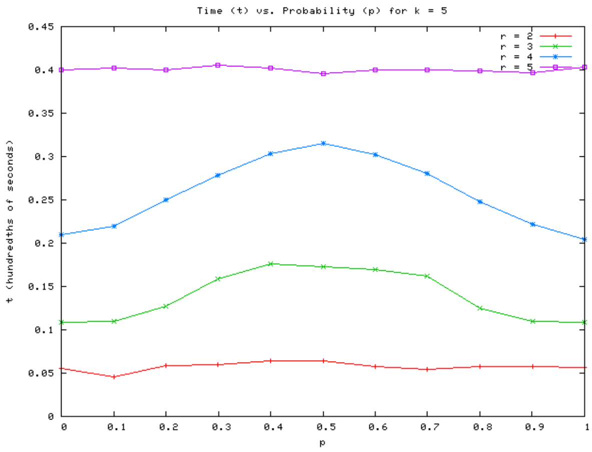

(a) $k = 5$

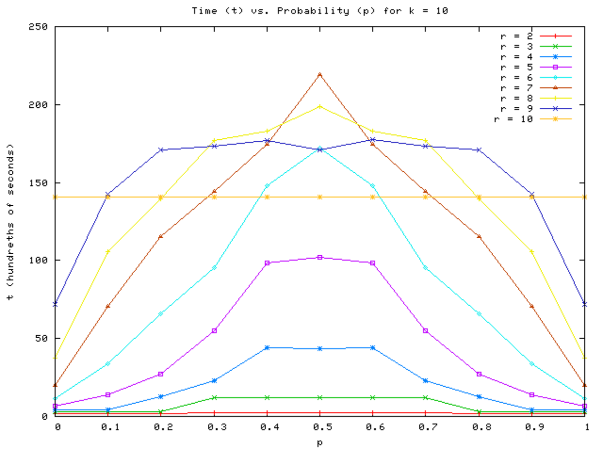

(b) $k = 10$

Figure 6: Plots of running time (t) vs. k for fixed values of the probability p.

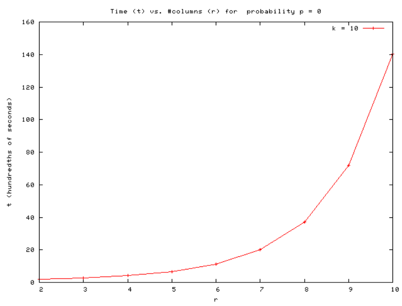

(a) $p = 0$

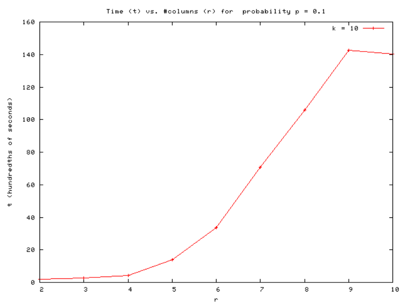

(b) $p = 0.1$

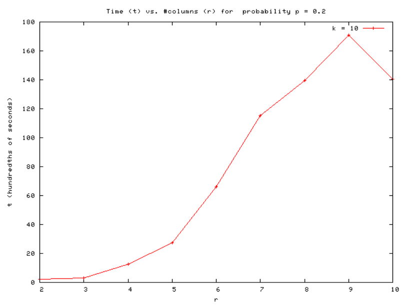

(c) $p = 0.2$

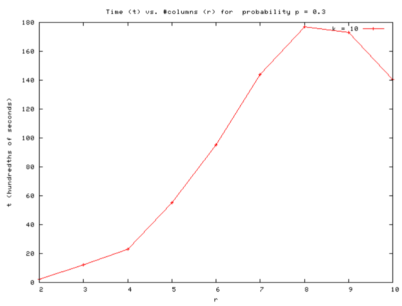

(d) $p = 0.3$

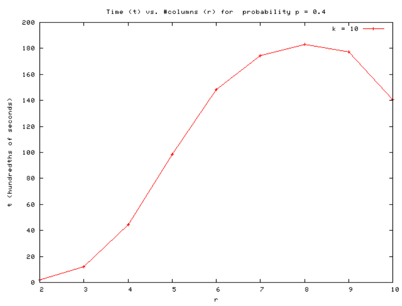

(e) $p = 0.4$

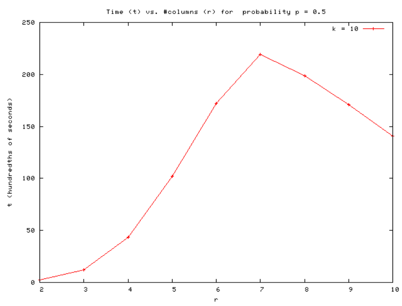

(f) $p = 0.5$

Figure 7: Plots of running time (t) vs. the probability p for fixed values of r.

ponent to the running time starts decreasing dramatically for $r \geq 7$. The exact relationship between these components is worth further study.

Scalability. Finally, we examined the scalability of our algorithm as dataset size increases. Recall that as k increases linearly from 5 to 20, the number of rows in the matrix increases exponentially in k. We focus on smaller values of r (in particular two and three) so as to make the dependence of running time on dataset size more explicit. Figure 8(a) and (b) show the dependence on running time for $r = 2$ and values of $p = 0.1$ and $p = 0.5$, respectively. The y-axis in these figures is on a logarithmic scale. Observe that p has negligible effect and that the running time mirrors the exponential growth in dataset size. Figure 8(c) and (d) show the dependence on running time for $r = 3$ and values of $p = 0.1$ and $p = 0.5$, respectively. Although we observe the same trends in each of the last two graphs, note that for $r = 3$ and $p = 0.5$, the algorithm runs an order of magnitude slower (the range of the y-axis in Figure 8(c) is $[0, 10^4]$ while the range in Figure 8(c) is $[0, 10^5]$). This observation reinforces the breakdown of running time into two components, in particular the role played by sparsity.

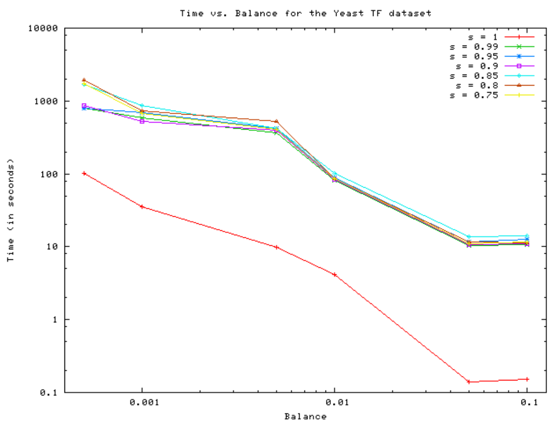

(a) Running time t vs. balance threshold b for fixed values of the support threshold s.

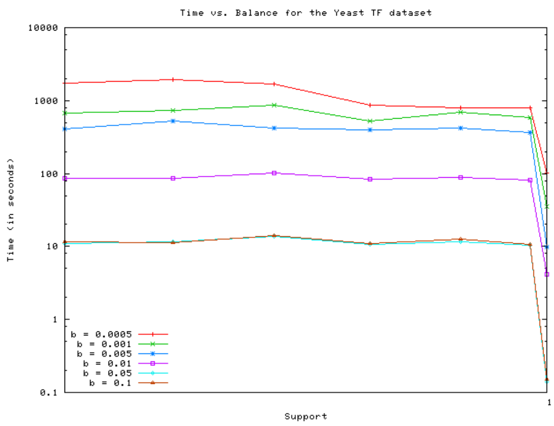

(b) Running time t vs. support threshold s for fixed values of the balance threshold b.

Figure 9: Performance of the truth table mining algorithm on the *S. cerevisiae* TF dataset.

6.2 Combinatorial Regulatory Networks

Gene expression in eukaryotic cells is controlled by the combinatorial interaction of transcription factors (TFs) and their binding motifs in DNA [2]. TFs often operate hierarchically: master regulators govern gene expression in multiple conditions, and act combinatorially with tissue- or condition-specific TFs to modulate gene expression. Truth tables representing TFs and the genes they regulate promise to capture the complexity of combinatorial regulation in eukaryotic cells.

To investigate this possibility, we analyzed a dataset of transcriptional regulation in *S. cerevisiae* [7] (baker's yeast). The dataset is a binary matrix whose columns represent 112 transcription factors and whose rows represent 4603 genes in *S. cerevisiae*; the matrix contains 12804 non-zero entries. A matrix entry contains a one if a ChIP-on-chip experiment indicates that the transcription factor binds to the promoter of the gene with a p-value at most 0.001. Although ChIP-on-chip data is noisy and significant effort may be needed to clean it up, the analysis we present next demonstrates that truth tables in such datasets can provide useful biological insights.

We ran our truth table finding algorithm on this dataset for balance values of $0.1, 0.05, 0.01, 0.005, 0.001$, and 0.0005 and support values of $1, 0.99, 0.95, 0.9, 0.85, 0.8$, and 0.75. Figure 9(a) displays on a log-log plot how the running time of the algorithm depends on the balance threshold we use. Each curve is this plot corresponds to a fixed value of support. We see that the logarithm of the running time is inversely proportional to the logarithm of the balance, for any given value of support. The plots also indicate that the case $s = 1$ requires less effort from the algorithm than values of support less than 1. Figure 9(a) displays on a log-log plot how the running time of the algorithm depends on the support threshold we use. As long as the support is less than 1, changing it does not have an adverse affect on the running time of the algorithm.

We mined truth tables by executing our algorithm on this data with $b = 0.001$ and $s = 0.75$. Our algorithm computed 6105 two-TF, 60570 three-TF, 6298 four-TF, and nine five-TF truth tables. We further examined the five-TF truth tables. One truth table includes the TFs CIN5, PHD1, RAP1, SKN7, and SWI4. The other eight truth tables involved various combinations of seven TFs: ACE2, FKH2, MBP1, NDD1, SKN7, SWI4, and SWI6. Note that the two sets share the TFs SKN7 and SWI4.

We first discuss the truth table involving RAP1, PHD1, CIN5, SWI4, and SKN7 in detail. PHD1 and SKN7 are TFs that regulate different aspects of cell growth. SWI4 is a key TF regulating the G1/S transition of the mitotic cell cycle. RAP1 is involved in chromatin silencing. SKN7 responds to different types of osmotic and oxidative stress while CIN5 is responsible for inducing the cell's response to drugs. The presence of all five TFs in a truth table suggests an intricate process of regulation that governs how the cell responds to external agents of stress potentially by shutting down the cell cycle and controlling its growth.

The truth tables that include ACE2, FKH2, MBP1, NDD1, SKN7, SWI4, and SWI6 shed light on other aspects of cellular growth and cell cycle control. FKH2 and NDD1 regulate G2/M-specific transcription in the mitotic cell cycle whereas ACE2 controls G1-specific transcription. MBP1 regulates progression through the cell cycle and is involved in DNA

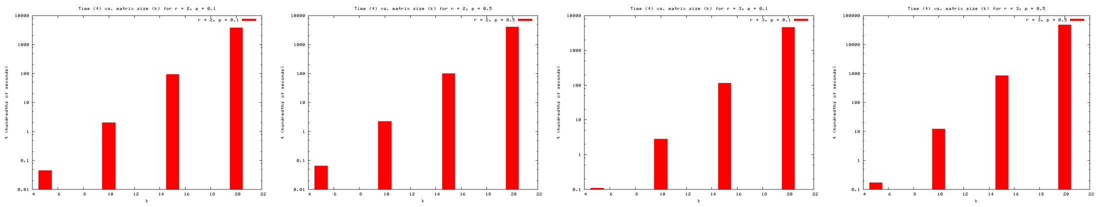

(a) $r = 2, p = 0.1$ (b) $r = 2, p = 0.5$ (c) $r = 3, p = 0.1$ (d) $r = 3, p = 0.5$

Figure 8: Plots of running time (t) vs. k for fixed values of the probability p.

replication. The shared membership of SKN7 and SWI4 in both groups of truth tables leaves open the possibility that as we discover more relationships between TFs and target genes, we may detect truth tables involving all ten TFs, thus coming closer to a more complete picture of transcriptional regulation in conditions of external stress.

6.3 Voting Dimensions of U.S. Senators

We also applied our truth table finding algorithm to voting patterns of the U.S. Senate. In particular, we obtained the roll call votes for first session of the 102nd Congress in 1991 from the Thomas database at the Library of Congress. This data contains the votes of 101 senators on 280 bills. A roll call vote guarantees that every senator's vote is recorded. We considered a "yes" vote to be a 1 and "no" vote or an abstension to be a 0.

When we used $b = 0.01$, and $s = 1$, all truth tables we mined had five or fewer bills. We used the χ^2 test to assess the independence of the bills in a truth table. Of the 60481 five-bill truth tables we found, 17976 were significant at the 0.01 level. We selected one of these significant truth tables at random to qualitatively assess the independence of the bills in it. The truth table we chose contained the bills

1 Nunn Resolution Re: Persian Gulf - S.J. Res. 1; A joint resolution regarding United States policy to reverse Iraq's occupation of Kuwait.

16 Dodd Amdt. No. 11; To amend the Export-Import Bank Act of 1945

39 Motion To Table S. Amdt. 59; To eliminate or reduce certain appropriations.

133 Byrd amdt.; To provide for an equalization in certain rates of pay, to apply the honoria ban and the provisions of title V of the Ethics in Government Act of 1978 to Senators and officers and employees of the Senate, and for other purposes

267 Motion To Table D'Amato Amendment No. 1405; To amend the Harmonized Tariff Schedule of the United States to clarify the classification of certain motor vehicles

These bills span diverse aspects of the political landscape: war, banking, pork, ethics, and trade.

We also counted the frequency of occurrence of each bill in significant truth tables. Interestingly, the five most frequent bills—39, 66, 97, 267, and 279—form a truth table themselves! Notice that we have already encountered bills 39 and 267. The subjects of the other three bills are the following:

66 Moynihan Amdt. No. 249; To amend the Ethics in Government Act of 1978 to apply the limitations on outside earned income to unearned income.

97 Motion To Table Amdt. No. 358; To eliminate language which lowers the Federal share payable for certain projects

279 Conference Report; Comprehensive Deposit Insurance Reform and Taxpayer Protection Act of 1991

In addition to war (bill 39) and trade (bill 267), these bills pertain to ethics, pork, and insurance reform. Such patterns shed direct light on the weighty deliberations that occupied the members of the 102nd Congress.

7. RELATED WORK

As stated earlier, truth tables form the anti-pattern to many concepts studied by other researchers. Brin et al. [16] were one of the first groups to find correlated sets of (binary) attributes using the χ^2 significance test. The TAPER algorithm [21] uses the Pearsons correlation metric instead; this work employs a upper bound on the correlation coefficient (for binary variables) to expose monotonicity constraints [21] that are useful for conducting all-pairs queries.

Truth tables with k properties, balance $\lfloor 1/2^k \rfloor$, and support 1 can be viewed as a special case of dense itemsets (defined in [15]) where the density is 50%. Observe, however, that, the density is of a particular nature and is more restrictive than the definition given by Seppanen and Mannila [15]. In particular, the form of density captured by a truth table obeys anti-monotonicity constraints without defining it as a statistic over densities of all its constituent sub-truth tables (as is done with the definition of weak density [15]). In general, the sparsity constraints of truth tables can be viewed as a sophisticated intersection statistic [14] over all (conjunctive) boolean expressions over the truth table's columns.

Truth tables are inherently also related to approaches that seek to quantify independence in binary datasets, e.g., Pavlov et al. [12] (whose end goal is to approximate answers to complex queries) and those that assess the dimensionality of the underlying dataset, e.g., Tatti et al. [17] by counting the number of independent columns. In fact, our work can be generalized into yielding graphical models for binary data [18]. One of the critical issues in building such models is identifying subsets of variables that induce conditional independence constraints. To support such analyses, we can generalise our definition of truth tables to *conditional truth tables* i.e., a truth table that surfaces only in a subset of the given data.

The partition of the rows of a truth table into distinct blocks with sufficient balance each is reminiscent of the work by Gionis et al. [5] that aims to identify subsets of rows and columns with a certain level of sparsity. Viewed in light of this work, a truth table is a patchwork of combinatorial rectangles each with a characteristic level of sparsity. However, as mentioned earlier, by exploiting properties that are satisfied by truth tables (but not combinatorial tiles in general), we are able to design effective algorithms.

8. DISCUSSION

We have formulated the novel data mining problem of finding truth tables in a binary matrix. In the continuum of informative patterns, truth tables reside at the end opposite that where itemsets and association rules lie, since truth tables represent properties that have no depenency patterns between them. The levelwise nature of the proposed mining algorithm means that we can employ many optimizations originally defined for *Apriori*-like algorithms, such as bounding the number of possible candidate patterns at a certain level based on the number of frequent patterns at the level below it [4].

The notion of truth tables displaying 50% sparsity in a characteristic manner deserves further study. For instance, the theoretical question of feasibility of identifying truth tables can be posed under given distributional assumptions (e.g., a Zipf distribution of the 0-1 data). We also intend to explore further the relationships between truth table mining and redescription mining toward designing dual-mining approaches.

9. REFERENCES

[1] R. Agrawal and R. Srikant. Fast Algorithms for Mining Association Rules in Large Databases. In *Proceedings of the 20th International Conference on Very Large Data Bases (VLDB'94)*, pages 487–499, Sep 1994.

[2] L. O. Barrera and B. Ren. The transcriptional regulatory code of eukaryotic cells–insights from genome-wide analysis of chromatin organization and transcription factor binding. *Curr Opin Cell Biol*, 18(3):291–8, 2006.

[3] J.B. Fitzgerald, B. Schoeberl, U.B. Nielsen, and P.K. Sorger. Systems Biology and Combination Therapy in the Quest for Clinical Efficacy. *Nature Chemical Biology*, Vol. 2(9):458–466, Sep 2006.

[4] F. Geerts, B. Goethals, and J.V.D. Bussche. Tight Upper Bounds on the Number of Candidate Patterns. *ACM Transactions on Database Systems*, Vol. 30(2):pages 333–363, June 2005.

[5] A. Gionis, H. Mannila, and J.K. Seppanen. Geometric and Combinatorial Tiles in 0-1 Data. In *Proceedings of the 8th European Conference on Principles and Practice of Knowledge Discovery in Databases (PKDD'04)*, pages 173–184, 2004.

[6] K. Goldberg, T. Roeder, D. Gupta, and C. Perkins. Eigentaste: A Constant Time Collaborative Filtering Algorithm. *Information Retrieval*, Vol. 4(2):pages 133–151, July 2001.

[7] Tong Ihn Lee, Nicola J. Rinaldi, Francois Robert, Duncan T. Odom, Ziv Bar-Joseph, Georg K. Gerber, Nancy M. Hannett, Christopher T. Harbison, Craig M. Thompson, Itamar Simon, Julia Zeitlinger, Ezra G. Jennings, Heather L. Murray, D. Benjamin Gordon, Bing Ren, John J. Wyrick, Jean-Bosco Tagne, Thomas L. Volkert, Ernest Fraenkel, David K. Gifford, and Richard A. Young. Transcriptional Regulatory Networks in Saccharomyces cerevisiae. *Science*, 298(5594):799–804, 2002.

[8] D.-I. Lin and Z.M. Kedem. Pincer-Search: An Efficient Algorithm for Discovering the Maximum Frequent Set. *IEEE Transactions on Knowledge and Data Engineering*, Vol. 14(3):553–566, 2002.

[9] S.C. Madeira and A.L. Oliveira. Biclustering Algorithms for Biological Data Analysis: A Survey. *IEEE/ACM Transactions on Computational Biology and Bioinformatics*, Vol. 1(1):24–45, Jan 2004.

[10] M. Natarajan, K.-M. Lin, R.C. Hsueh, P.C. Sternweis, and R. Ranganathan. A Global Analysis of Cross-talk in a Mammalian Cellular Signaling Network. *Nature Cell Biology*, Vol. 8(6):571–580, June 2006.

[11] L. Parida and N. Ramakrishnan. Redescription Mining: Structure Theory and Algorithms. Technical report, Feb 2005.

[12] D. Pavlov, H. Mannila, and P. Smyth. Beyond Independence: Probabilistic Models for Query Approximation on Binary Transaction Data. *IEEE Transactions on Knowledge and Data Engineering*, Vol. 15(6):pages 149–1421, 2003.

[13] N. Ramakrishnan, D. Kumar, B. Mishra, M. Potts, and R.F. Helm. Turning CARTwheels: An Alternating Algorithm for Mining Redescriptions. In *Proceedings of the Tenth ACM SIGKDD International Conference on Knowledge Discovery and Data Mining (KDD'04)*, pages 266–275, Aug 2004.

[14] J.K. Seppanen. *Using and Extending Itemsets in Data Mining*. PhD thesis, 2006.

[15] J.K. Seppanen and H. Mannila. Dense Itemsets. In *Proceedings of the Tenth ACM SIGKDD International Conference on Knowledge Discovery and Data Mining (KDD'04)*, pages 683–688, Aug 2004.

[16] C. Silverstein, S. Brin, and R. Motwani. Beyond Market Baskets: Generalizing Association Rules to Dependence Rules. *Data Mining and Knowledge Discovery*, Vol. 2(1):pages 39–68, 1998.

[17] N. Tatti, T. Mielikainen, A. Gionis, and H. Mannila. What is the Dimension of your Binary Data? In *Proceedings of the 6th IEEE International Conference on Data Mining (ICDM'06)*, pages 603–612, 2006.

[18] J.L. Tuegels and J.V. Horebeek. Generalized Graphical Models for Discrete Data. *Statistics and Probability Letters*, Vol. 38:41–47, May 1998.

[19] List of newspeak words. Wikipedia. http://en.wikipedia.org/wiki/List_of_Newspeak_words#Bellyfeel.

[20] Truthiness. Wikipedia. http://en.wikipedia.org/wiki/Truthiness.

[21] H. Xiong, S. Shekhar, P.-N. Tan, and V. Kumar. TAPER: A Two-Step Approach for All-Strong-Pairs Correlation Query in Large Databases. *IEEE Transactions on Knowledge and Data Engineering*, Vol. 18(4):pages 493–508, 2006.

[22] M.J. Zaki and N. Ramakrishnan. Reasoning about Sets using Redescription Mining. In *Proceedings of the Eleventh ACM SIGKDD International Conference on Knowledge Discovery and Data Mining (KDD'05)*, pages 364–373, Aug 2005.